J Math Chem (2009) 46:942–951
DOI 10.1007/s10910-009-9555-z

ORIGINAL PAPER

Mixed silicon–germanium nanocrystals: a detailed study of Si_xGe_{47-x}:H

A. D. Zdetsis · C. S. Garoufalis · E. N. Koukaras

Received: 6 September 2006 / Accepted: 30 September 2008 / Published online: 10 July 2009

Abstract Mixed SiGe:H nanocrystals have been studied within the framework of Density Functional Theory. (DFT) using the hybrid non-local exchange-correlation functional of Becke, Lee, Parr and Yang (B3LYP). In addition to ground-state DFT/B3LYP calculations, excited-state calculations for the determination of the optical absorption spectrum have been performed employing the time-dependent density functional theory (TDDFT). In order to fully investigate the substitution of Si by Ge, on structural, cohesive, electronic and optical properties, we have used the Si_xGe_{47-x}:H nanocrystal, as a representative medium size nanosystem. Our results show that the optical gap depends not only on the relative concentrations of silicon, germanium and hydrogen, but also on the relative position of the silicon and germanium shells relative to the surface of the nanocrystal. This is also true for the structural, cohesive and electronic properties. This dependence allows for the possibility of electronic and optical gap engineering.

Keywords Nanocrystals · Nanoparticles · Optical gap · Density functional theory

1 Introduction

The possibility of tunable photoluminescence from silicon and silicon-like (e.g., germanium) nanocrystals, as well as from porous silicon, p-Si, composed of Si nanocrystals, has stimulated intensive research on this type of materials over the last decade [1–21]. Until recently [17–21], silicon nanocrystals have practically "monopolized" the interest of the researchers. A large portion of this type of work has been devoted to understanding the visible photoluminescence of these materials and its dependence on the diameter of the nanoparticles (or equivalently, the porosity of p-Si). It is

A. D. Zdetsis (✉) · C. S. Garoufalis · E. N. Koukaras
Department of Physics, University of Patras, 26500 Patras, Greece
e-mail: zdetsis@upatras.gr; zdetsis@physics.upatras.gr

widely accepted and well established by now (see for instance Ref. [14–17]) that the luminescence of unreconstructed oxygen-free Si nanocrystals (of well defined diameter) is mainly due to quantum confinement of the corresponding nanoparticles. This is also true for Ge nanoparticles and porous germanium [17–20].

By varying the diameters of the nanocrystals (or equivalently the porosity of porous silicon) intense PL can be obtained across the visible spectrum, which could never have taken place for bulk crystalline silicon with a band gap of 1.2 eV. Quantum confinement is responsible for the opening of the gap in silicon from the 1.2 eV bulk value, to values of 6–7 eV (for small nanocrystals). For larger nanocrystals (larger than 2.5 nn) the enlarged gap falls into the visible region of the spectrum (2–3 eV), while for even larger (larger than about 4 nm) the optical gap falls below the visible range. These large values of the gap for small size nanocrystals, obviously are equally undesirable for optical applications as the shrinking of the gap for larger nanocrystals and bulk silicon.

One way of adjusting the gap to desired values is the size of nanocrystals (or the porosity in p-Si). The other obvious way is substitution of Si atoms by different atoms with similar properties (Ge) or doping. Here we will examine the first possibility. It is anticipated that the effect of over-opening of the gap at small sizes of nanocrystals would not be so strong for Ge nanocrystals [19] due to the smaller band gap of bulk Ge, compared to bulk Si. However, if we consider only pure germanium hydrogenated nanocrystals, the possibilities of adjusting the optical gap (and the band gap) are limited only to proper size selection (if we ignore reconstruction or oxygen contamination). The possibility of combining the advantages of Si (in the electronic properties) with those of Ge (especially structural and mechanical properties) is an intriguing and very promising possibility, for the development of optoelectronic nanodevices. Needless to say, that, not only the minimum critical diameter of the nanocrystals for visible PL is important, but also the maximum possible diameter. With this in mind, we have examined the optical and electronic properties of mixed nanocrystals of the form $Si_xGe_y:H_z$, where z is determined by the sum of $x + y$. For the particular case of $Si_xGe_{47-x}:H_{60}$ nanocrystals we have studied in detailed the variation of the cohesive, electronic and optical properties as a function of x.

2 Technical details of the calculations

All calculations in this work are based on time dependent density functional theory (TDDFT) [22] employing the nonlocal exchange-correlation functional of Becke, Lee, Yang and Parr (B3LYP) [23]. The accuracy of these calculations (TDDFT/B3LYP) for the optical gap has been tested before by high level multireference second-order perturbation theory (MR-MP2) for the case of Si nanocrystals, with excellent results [15].

The size of the nanocrystals considered here ranges from 5 to about 20 Å. This corresponds to values of x and y from 5 to 99 Si or Ge atoms and to values of z between 12 and 100 H atoms (a total of about 199 atoms). The symmetry of the nanocrystals is T_d and their geometries have been fully optimized within this symmetry constraint using the hybrid B3LYP functional. To preserve the T_d symmetry, we substituted shells of silicon (rather than isolated atoms) by equivalent germanium shells. This

choice introduces an additional restriction on the variation of Si concentration. The optical gap, for the nanocrystals constructed in this way, was calculated using the time-dependent density functional method [22], B3LYP/TDDFT, as the energy of the first allowed electronic excitation (within the T_d symmetry constrain). The optical gap and the electronic density of states (DOS), was calculated for a large variety of nanocrystals.

For the particular case of Si_xGe_{47-x}:H_{60}, we have examined in detailed most of the structural (bond length distribution), cohesive (binding energies), electronic (DOS, electronic gaps) and optical (lower part of absorption spectrum) properties as a function of the concentration x. In addition, for the same concentration x we have considered alternative ways of substitution of the shells of silicon atoms by germanium.

The bulk of our calculations were performed with the TURBOMOLE [7] suite of programs using Gaussian atomic orbital basis sets of split valence [SV(P)]: [4s3p1d]/[2s] quality [11].

3 Results and discussion

3.1 Structural and cohesive properties

Representative geometries of Si_xGe_y:H_z nanoclusters are shown in Fig. 1 for various concentrations and substitutions, for the particular case of $x + y = 71$. The bonding characteristics of the various structures can be easily visualized and described graphically in a synoptic way, through the bond-length distributions. In Fig. 2 we present the bond-length distribution for the family of Si_xGe_{47-x}:H_{60} nanocrystals, for various values of x. As we can see in the figure the Si–Si distribution has a peak around 2.48 Å for the first shell of neighbours (connected to the central atom) and a second peak around the 2.37 Å for the rest of the silicon atoms. This second peak, corresponding to shorter bond-lengths by 0.1 Å, is more or less constant, with a tendency to approach the bulk value of 2.36 Å for larger nanocrystals. This is also true for Ge–Ge bonds. Comparing Fig. 2a and b we can see that in both cases the bonds of the central atom with the first shell of neighbours are longer by 0.1 Å. We also observe in Fig. 2e and f that there are no Ge–Ge bonds in the nanoparticles, although there is a significant amount of germanium atoms. This indicates that the particular germanium shells are bonded only to shells above or/and below, consisting of silicon atoms. As was explained earlier, with the same concentrations (x, y and z) more than one nanocrystals can be constructed. Moreover, since the Ge substitutions in the present work deal with spherical shells of neighbours rather than with individual atoms, we can distinguish two classes of nanocrystals with the same concentrations; those with the Ge atoms in the inner core, and those with the Ge atoms in the outer shells ("surface"). The structural and cohesive characteristics are different in the two cases. As we can see in Fig. 3, we have two distinct curves (parallel lines) depending on the exact location of the Ge layer relatively to the surface of the nanocrystals. It is clear from this plot that it is preferable to have the Ge atoms in the "inner" part of the nanocrystal. This tendency must be related with the effect of hydrogen. Without the hydrogen passivation of the dangling bonds, it would be natural (energetically favoured) for the Ge atoms to segregate onto the

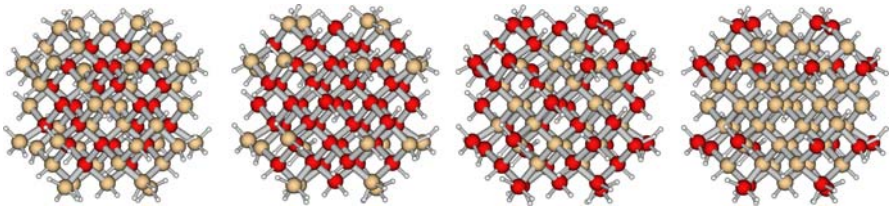

Fig. 1 A succession of Ge-layers depositions corresponding to the Si_xGe_y:H_z nanocrystal with $x + y = 71$

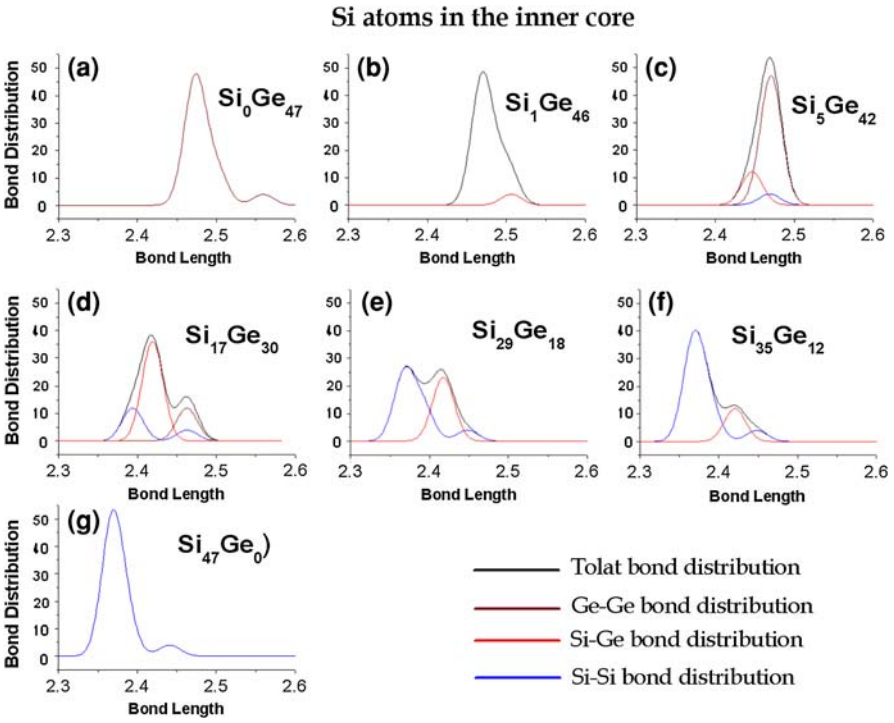

Fig. 2 Bond distribution in Si_xGe_{47-x}:H_{60} for x = 0, 1, 5, 17, 29, 35, 47. The Ge–Ge, Si–Ge and Si–Si bond distributions are shown separately. The constant number of the hydrogen atoms (60) is not shown in the graphs

surface in order to minimize the cost of the dangling bonds. Indeed, as was stated by Tarus et al. [24], for hydrogen-free SiGe nanoclusters, germanium tends to segregate onto the surface.

3.2 Electronic properties

In Fig. 4 we have plotted the density of states (DOS) for three typical nanocrystals (one Si-rich, one Ge-rich and one of about equal concentrations of Si and Ge). The DOS curves were generated from the eigenstates of the ground state calculations with

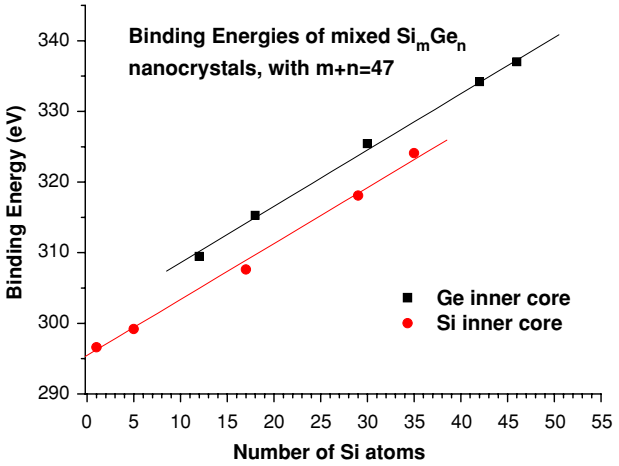

Fig. 3 Total binding energy as a function of the number of silicon atoms

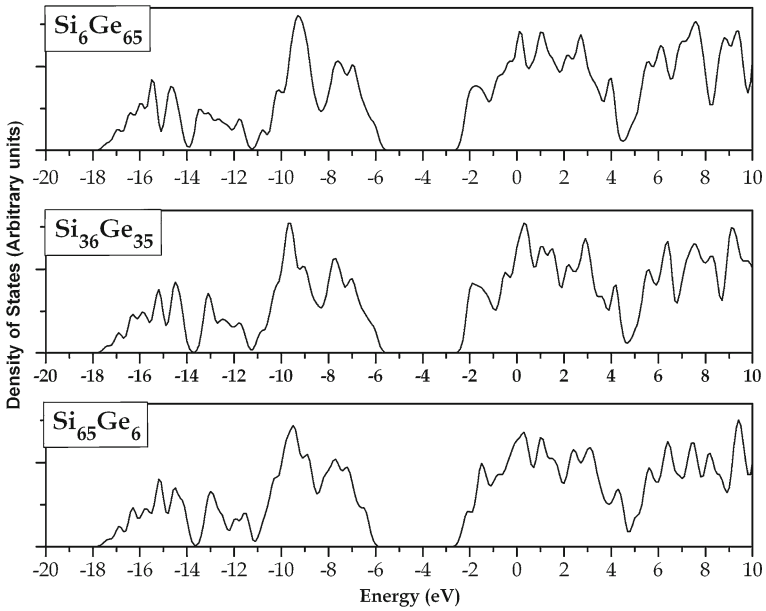

Fig. 4 Electronic density of states (DOS) of representative nanocrystals

a suitable gaussian broadening. Careful examination of the figure reveals that the largest variation with the Ge concentration occurs in the valence band edges, while the conduction band edge is relatively insensitive.

The "band structure" or DOS gap corresponds in real space to the energy separation of the highest occupied (HO) and lowest unoccupied (LU) molecular orbital (MO). The variation of the HOMO–LUMO gap as a function of x is shown in Fig. 5 for $Si_xGe_{47-x}:H_{60}$. This plot includes, for the same or similar concentration x, both types

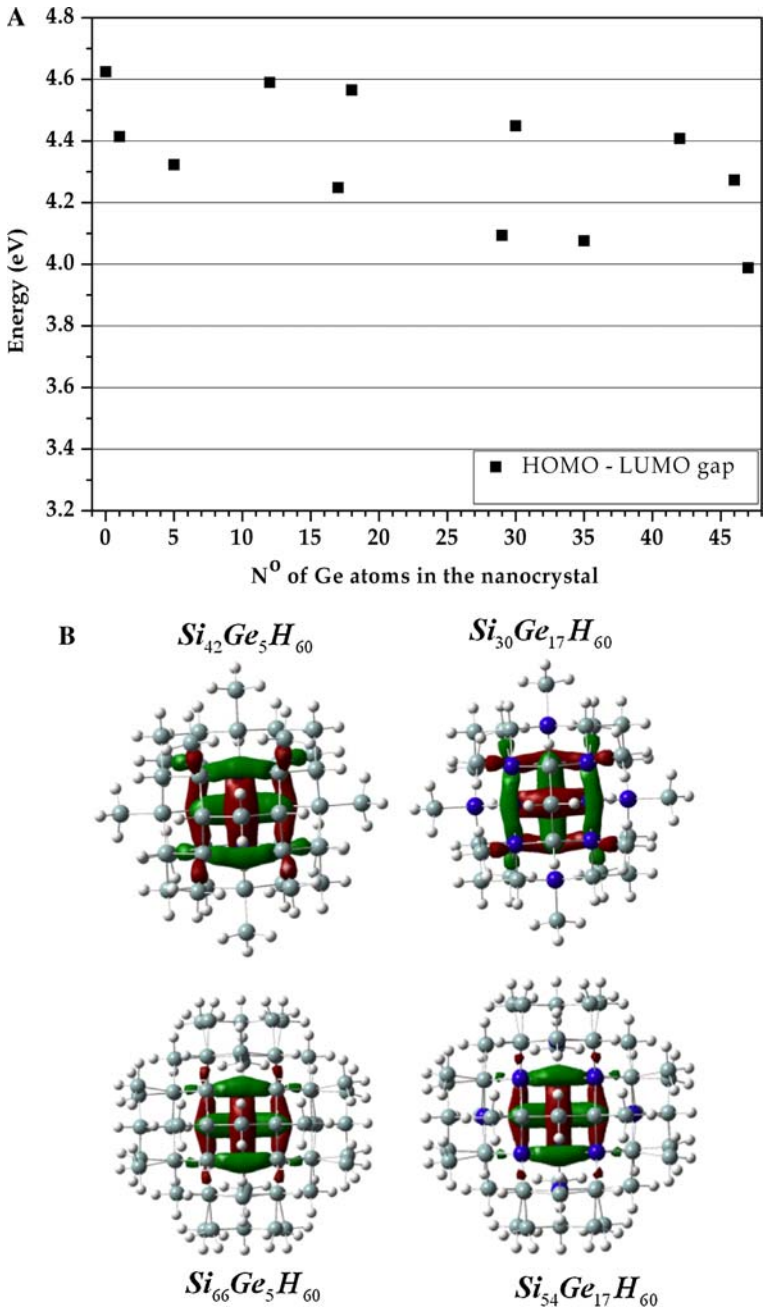

Fig. 5 (a) The HOMO–LUMO gap for Si_xGe_{47-x}:H_{60} nanocrystals, as a function of the number of Ge atoms ($47-x$). (b) The highest occupied molecular orbitals (HOMO) for several nanocrystals

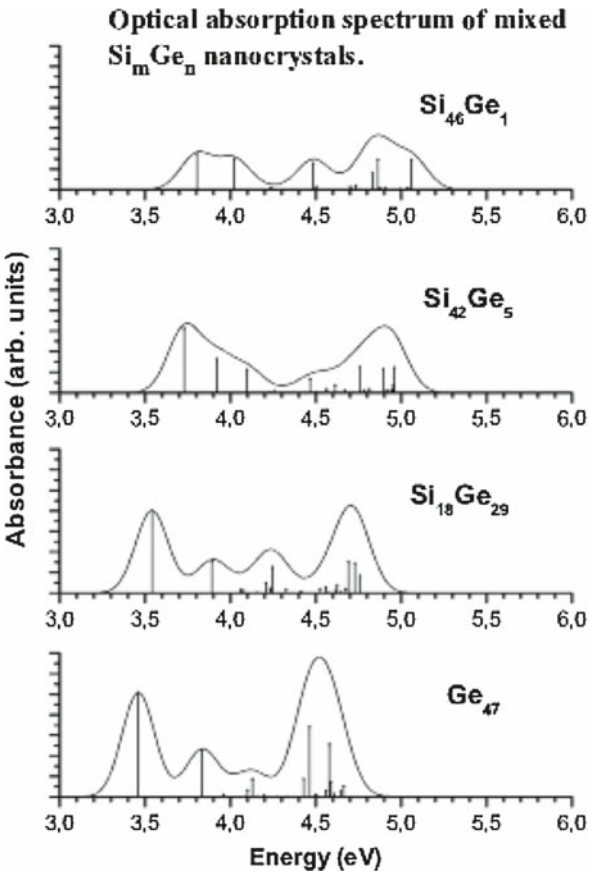

Fig. 6 The optical absorption spectrum of of $Si_xGe_{47-x}:H_{60}$ nanocrystals for $x = 0$, 18, 42, 46. The continuous lines are produced by a Gaussian broadening of the spectral lines

(inner and outer) of silicon substitution by germanium. We can distinguish clearly the two sets of points (disjoint curves). Surprisingly enough, the larger HOMO–LUMO gaps correspond to germanium atoms lying in the surface region, which as we have seen in Fig. 3 is not energetically as stable as the opposite case. For homogeneous similar molecular systems we would expect that the larger HOMO–LUMO gap would correspond to the structure of lowest energy. However, in cases where cohesion and reactivity are due to different mechanisms, this is not necessarily the case. Perhaps something similar is happening here. As we can see in Fig. 6, the HOMO orbitals are well localized around germanium sites, and therefore they are sensitive to the exact location of germanium shells. On the other hand, the LUMO orbitals, corresponding to the conduction band-edges, as we can see in Fig. 4, are relatively insensitive to the number and position of germanium atoms.

Calculations of the HOMO–LUMO gap of mixed $Si_xGe_y:H_z$ nanocrystals have also been recently performed by Yu et al. [21], specifically for nanocrystals with a total number of Si and Ge atoms of 71 ($x + y = 71$). These calculations are based on density-functional theory (DFT) in the local-density approximation (LDA). The resulting

HOMO–LUMO gaps range from 3.3 to 4.1 eV corresponding to the pure Ge and pure Si nanocrystals, while our results give 4.0 eV for the pure Ge nanocrystal and 4.6 eV for the pure Si nanocrystal. The small differences can be attributed to the use of LDA approximation which is known [13–17] to underestimate both the HOMO–LUMO and the optical gaps. Furthermore, the gap dependence on Ge concentration is practically linear in their work. The difference from the present results apparently is due to the different distribution of Ge atoms. Instead of shells of atomic neighbours, used in the present work, the Ge atoms in Ref. [21] are distributed more homogeneously, and they are allowed to diffuse through the shells.

3.3 Optical properties

In Fig. 6 we plot the excitation spectrum of Si_xGe_{47-x}:H_{60} nanocrystals as a function of x. The shrinking of the spectrum and of the optical gap is very clear as the content of germanium increases. This plot corresponds to germanium atoms in the interior of the nanocrystals.

The exact behaviour of the optical gap, for both types of substitutions is shown in Fig. 7. The values for the optical gap (for $x \neq 0$ or 47) are intermediate between those of pure Si and pure Ge. This is true for all sizes of nanocrystals. We observe that, in analogy to Fig. 5 for the HOMO–LUMO gap, we have an upper and a lower curve meeting at the end-points. The upper part of the curve, in analogy to the HOMO–LUMO gap, corresponds to germanium shells lying in the outer part of the nanocrystal. For a possible interpretation one could speculate that, since the lower portion of the curves corresponds to inner cores of germanium, one could expect that the gap would

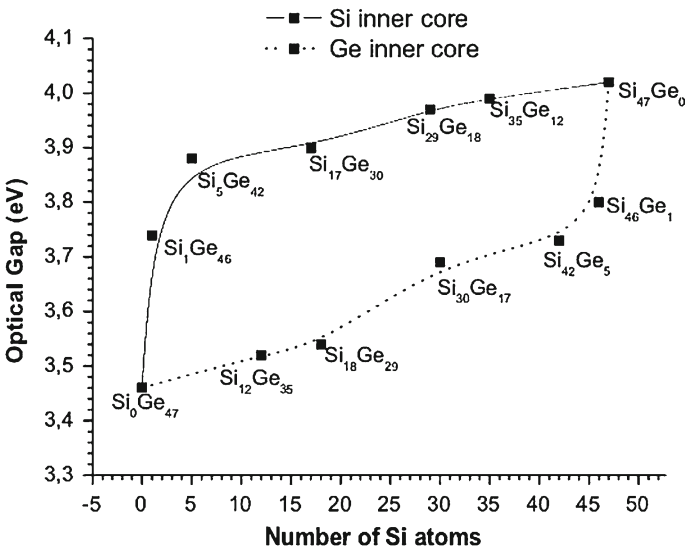

Fig. 7 The variation of the optical gap as a function of the number of silicon atoms, for the two categories of Si_xGe_{47-x}:H_{60} crystals

decrease with increasing core size (in agreement with quantum confinement). If this is the case, then the outer silicon shells would effectively play the role of surface passivants. Since quantum confinement is stronger for Ge than Si [21] (the effective Bohr radius of the exciton in Ge is larger than that in Si) the opposite arrangement would lead to weaker gap reduction and the net effect could be the "looping" curve of Fig. 7. Thus, in principle the gap (and the general properties) of these nanosystems could be adjusted not only with the size and the relative concentration of Si and Ge atoms, but also with the relative position of the atoms with respect to the surface.

4 Conclusions

We have shown that, indeed, the mixed SiGe nanocrystals have optical and electronic properties intermediate between those of pure Si and Ge nanocrystals. The large variety of optical and band gaps depends, not only on the size of the nanocrystals and the relative concentrations of Si and Ge, but also on the relative spatial distribution of the Ge atoms with respect to the surface of the nanocrystals. These added degrees of freedom in the future design of such (and similar) systems, could greatly enhance the possibility of electronic and optical gap engineering.

Acknowledgments We thank the European Social Fund (ESF), Operational Program for Educational and Vocational Training II (EPEAEK II), and particularly the Program PYTHAGORAS, as well as the University of Patras Research Committee (basic research program "K. KARATHEODORIS 2003") for funding the above work.

References

1. L.T. Canham, Appl. Phys. Lett. **57**, 1046 (1990)
2. J.P. Wilcoxon, P.P. Provencio, G.A. Samara, Phys. Rev. B **64**, 035417 (2001)
3. M.V. Wolkin, J. Jorne, P.M. Fauchet, G. Allan, C. Delerue, Phys. Rev. Lett. **82**, 197 (1999)
4. F.A. Reboredo, A. Franceschetti, A. Zunger, Phys. Rev. B **61**, 13073 (2000)
5. S.L. Schuppler et al., Phys. Rev. Lett. **72**, 2648 (1994)
6. S.L. Schuppler et al., Phys. Rev. B **52**, 4910 (1995)
7. M. Rohlfing, S.G. Louie, Phys. Rev. Lett. **80**, 3320 (1998)
8. S. Öğüt, J. Chelikowsky, S.G. Louie, Phys. Rev. Lett. **79**, 1770 (1997)
9. S. Öğüt, J. Chelikowsky, S.G. Louie, Phys. Rev. Lett. **80**, 3162 (1998)
10. L.E. Brus, P.F. Szajowski, W.L. Wilson, T.D. Harris, S. Schuppler, P.H. Citrin, J. Am. Chem. Soc. **117**, 2915 (1995)
11. K. Kim, Phys. Rev. B **57**, 13072 (1998)
12. S. Furukawa, T. Miyasato, Phys. Rev. B **38**, 5726 (1988)
13. Y. Kanemitsou, Phys. Rev. B **49**, 16845 (1994)
14. I. Vasiliev, J.R. Chelikowsky, R.M. Martin, Phys. Rev. B **65**, 121302-1 (2002)
15. C.S. Garoufalis, A.D. Zdetsis, S. Grimme, Phys. Rev. Lett. **87**, 276402 (2001)
16. A.D. Zdetsis, C.S. Garoufalis, S. Grimme, *Proceedings of NATO Advanced Research Workshop on "Quantum Dots: Fundamentals, Applications, and Frontiers" Crete, Greece* (Kluwer/Springer, Dordrecht/New York, 2005), pp. 317–332
17. A.D. Zdetsis, Rev. Adv. Mater. Sci. **11**, 56–78 (2006)
18. H.Ch. Weissker, J. Furthmuller, F. Bechstedt, Phys. Rev. B **65**, 155328 (2002)
19. C.S. Garoufalis, A.D. Zdetsis, J. Phys. Conf. Ser. **10**, 69 (2005)
20. A.D. Zdetsis, C.S. Garoufalis, M.S. Skaperda, E.N. Koukaras, J. Phys. Conf. Ser. **10**, 97 (2005)
21. M. Yu, C.S. Jayanthi, D.A. Drabold, S.Y. Wu, Phys. Rev. B **68**, 035404 (2003)

22. M.E. Casida, in *Recent Advances in Density Functional Methods*, vol. 1, ed. by D.P. Chong (World Scientific, Singapore, 1995)
23. P.J. Stephens, F.J. Devlin, C.F. Chabalowski, M.J. Frisch, J. Phys. Chem. **98**, 11623 (1994)
24. J. Tarus, M. Tantarimaki, K. Nordlund, Nucl. Instr. Meth. B **228**, 51–56 (2005)
25. TURBOMOLE (Version 5.6), Universitat Karlsruhe (2002)
26. A. Schäfer, H. Horn, R. Ahlrichs, J. Chem. Phys. **97**, 2571 (1992)